Supplemental Figure S1.

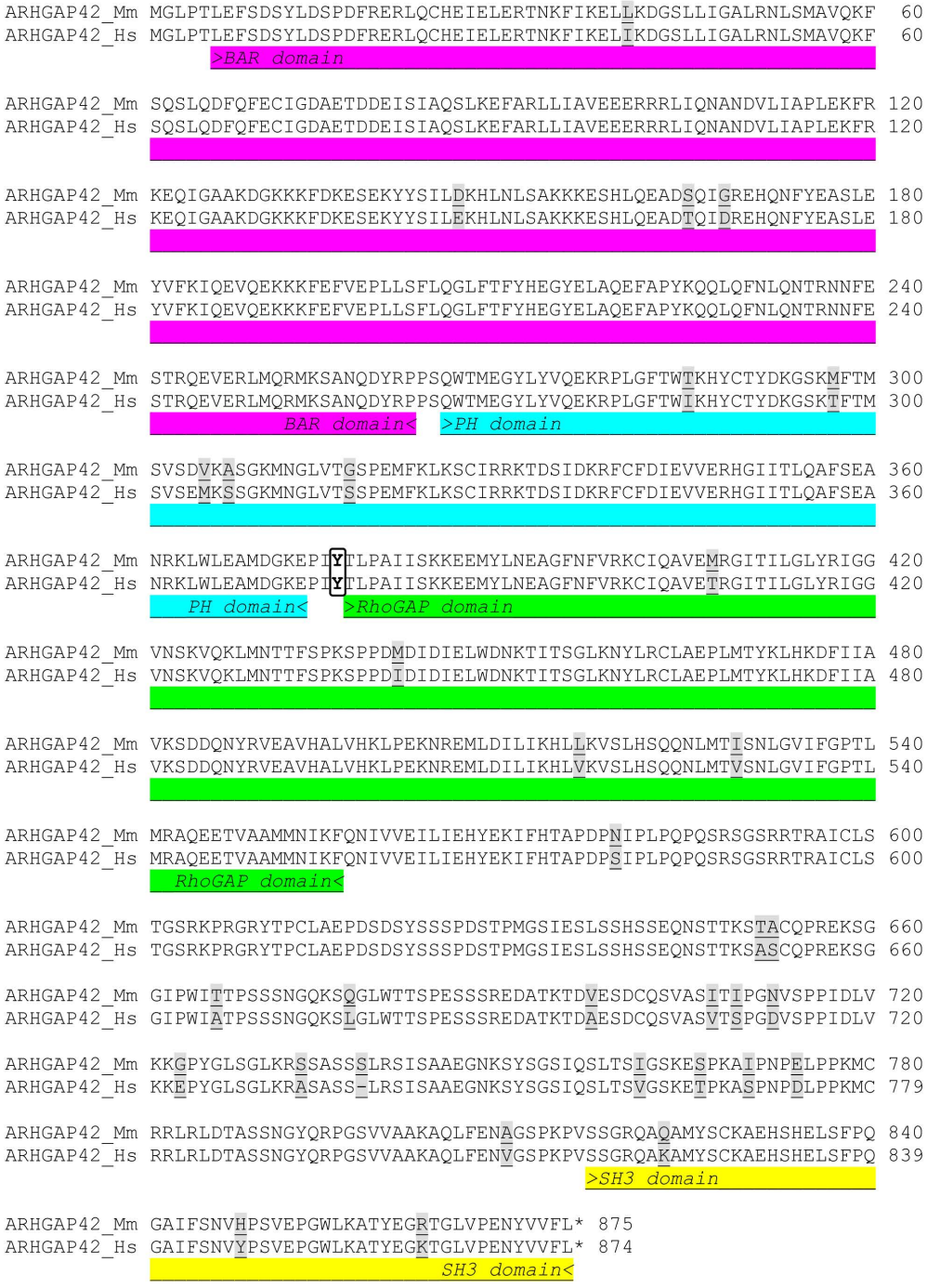

Supplemental Figure S1. Mouse *vs.* human ARHGAP42. Mouse ARHGAP42 (ARHGAP42_Mm) is shown aligned against the predicted human protein (ARHGAP42_Hs; UniProt accession number A6NI28). Non-identical residues are shaded. Asterisks indicate STOP codons. Numbers indicate amino acid position. Positions of BAR, PH, GAP, and SH3 domains are shown below the aligned sequences. The Tyr-376 phosphorylation site is in bold and indicated by a box. Note that the UniProt entry for mouse RhoGAP42 (accession number B2RQE8, not shown) is missing amino acid residues 129-162 within the BAR domain.

Supplemental Figure S2.

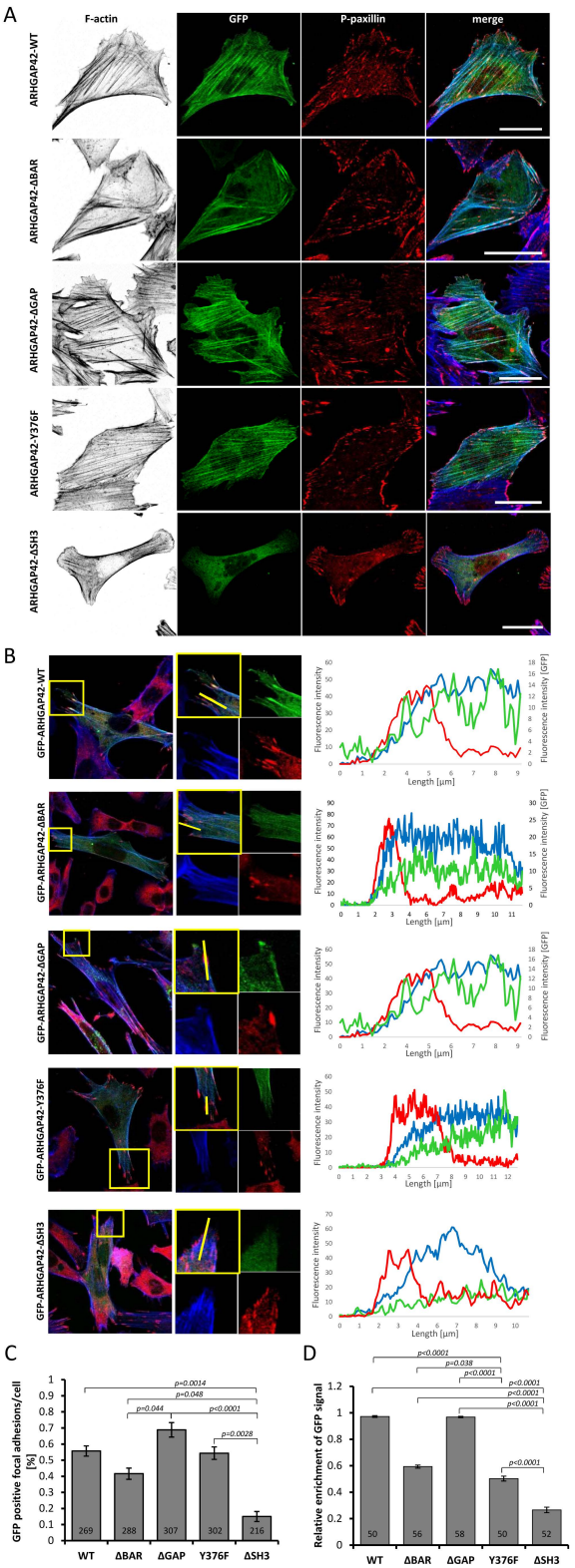

Supplemental Figure S2. Subcellular localization of ARHGAP42 mutational variants. (A) GFP-ARHGAP42 variants ΔBAR, ΔGAP, ΔSH3, and Y376F were expressed in MEFs and analyzed by fluorescence microscopy. The cells were immunostained with phalloidin to mark F-actin (in grey or blue), anti phospho-paxillin antibody to mark focal adhesions (in red) and GFP-ARHGAP42 variants were visualized by GFP fluorescence (in green). Scale bars are 30 µm. (B) Analysis of GFP-ARHGAP42 variants localization to focal adhesions. MEFs expressing indicated ARHGAP42 variants were prepared and immunostained as described above. Graphs on the right from the images show the fluorescence intensity profiles analyzed in a longitudinal section (indicated by the yellow line) through focal adhesion. (C) The bar graph shows the percentage of focal adhesions enriched in presence of indicated GFP-ARHGAP42 variant. (D) The bar graph shows statistical analysis of relative enrichment of indicated GFP-ARHGAP42 variants in longitudinal sections through focal adhesions. The relative enrichment was calculated as a ratio of length given by the presence of GFP signal in a longitudinal section through focal adhesion (as shown in B)) and length of the focal adhesion (defined by the P-paxillin signal). Only focal adhesions positive to GFP-ARHGAP42 signal were analyzed. (C, D) Numbers in the histogram bars indicate number of focal adhesions analyzed. Error bars represent standard errors. Statistical significances were determined by one-way ANOVA followed by Tukey's post-hoc test.

Supplemental Figure S3.

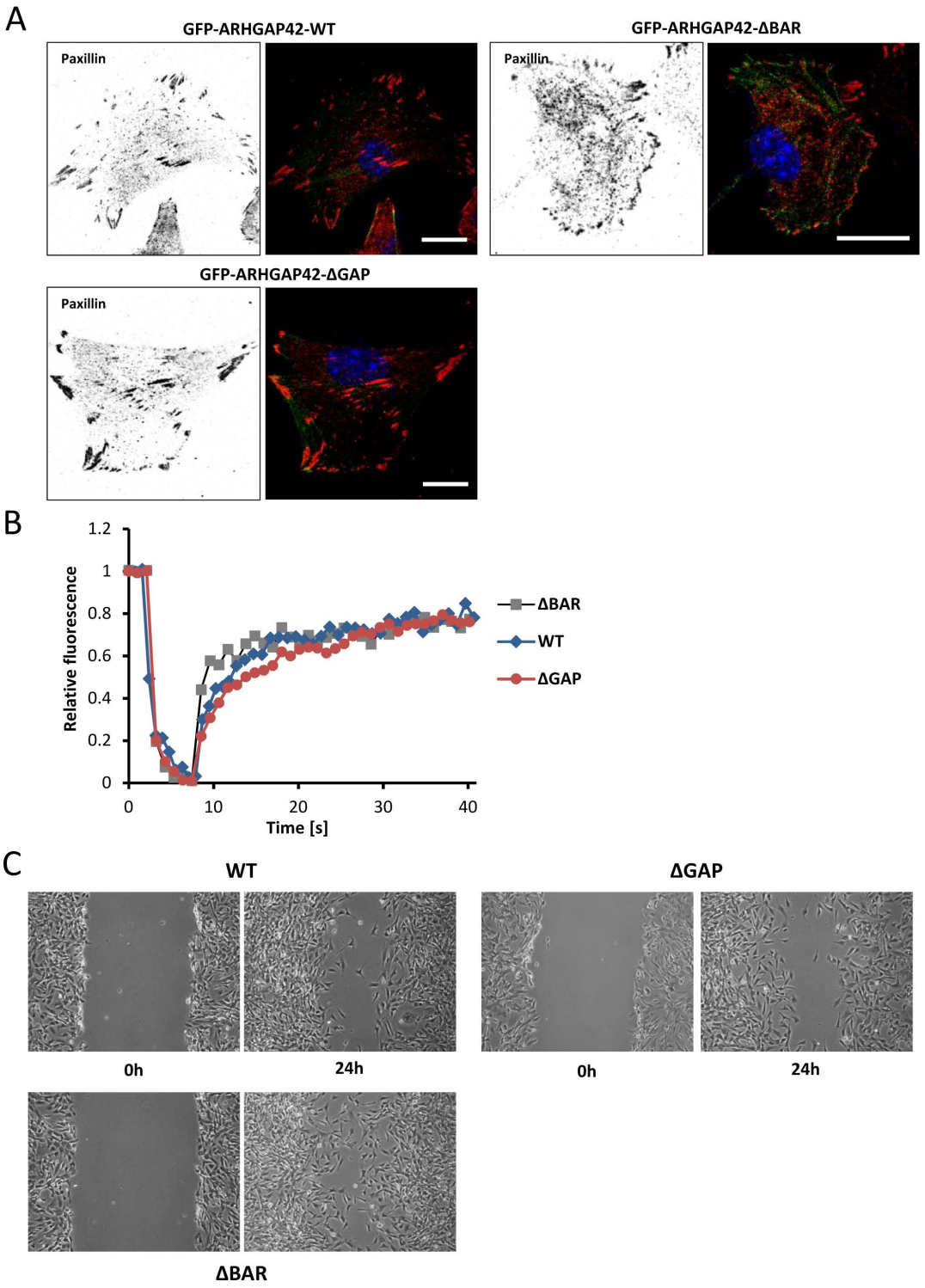

Supplemental Figure S3. Expression of ARHGAP42-ΔGAP increases the size of focal adhesions. MEFs stably expressing GFP-ARHGAP42 variants (WT, ΔBAR, ΔGAP) were grown on fibronectin-coated cover slips, fixed and focal adhesion size was analyzed by fluorescence microscopy. The cells were immunostained with an antibody against paxillin to mark focal adhesions. (A) Representative images showing focal adhesions stained by paxillin; left: greyscale signal of paxillin, right: merge (blue: DAPI, green: GFP, red: Paxillin). Scale bars are 20 µm. (B) Representative FRAP curves of mCherry-Vinculin dynamics in focal adhesions in MEFs expressing indicated variants of ARHGAP42. (C) Representative images of monolayer wound healing of MEFs expressing GFP-ARHGAP42 variants WT, ΔBAR, and ΔGAP.

Supplemental Figure S4.

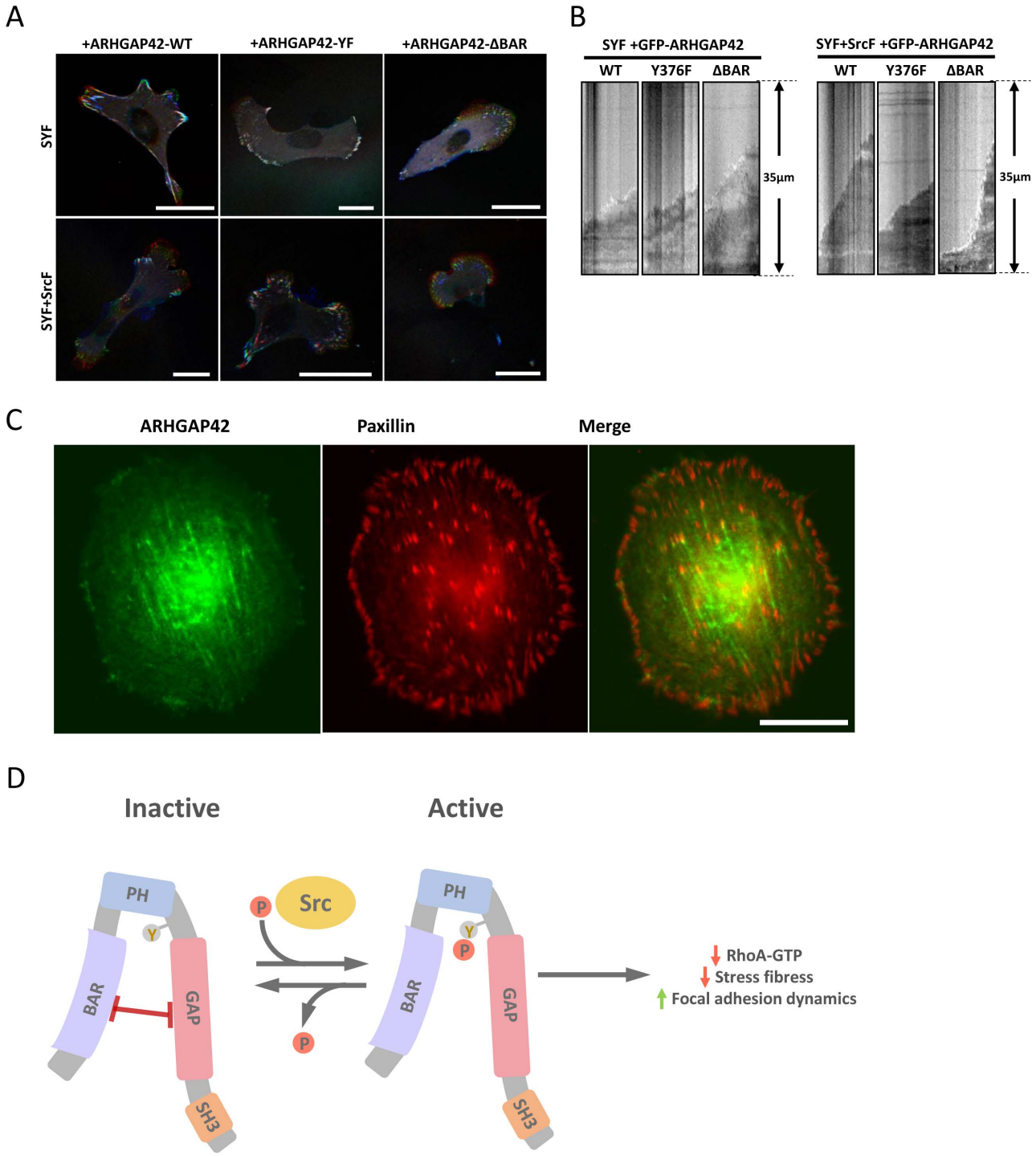

Supplemental Figure S4. (A, B) Src phosphorylation of ARHGAP42 on Tyr376 regulates focal adhesion and lamellipodial dynamics. SYF cells or SYF cells expressing constitutively active Src (SrcF) were co-transfected with GFP-ARHGAP42 expression plasmids (WT, Y376F, and ΔBAR). Cells were plated on fibronectin covered glass bottom dishes and after 24 hours cells showing similar levels of GFP-ARHGAP42 fluorescence, judged using an integrated intensity value of the GFP signal per cell and acquired with same settings (exposure, laser power, detector gain, etc.) of the microscope, were analyzed by confocal live cell microscopy. (A) Representative color-coded images of cell expressing ARHGAP42 variants observed for 10 min. Color coding: 0 min – blue, 5 min – green, 10 min – red; dynamic adhesions are colored and stable adhesions are white. (B) Representative kymographs of protruding lamellipodia showing increased lamellipodium velocity in cells with increased ARHGAP42 activity. **(C) Subcellular localization of endogenous ARHGAP42.** MEFs were immunostained with ARHGAP42 antibody (green, endogenous ARHGAP42) and anti-Paxillin (red) antibody to mark focal adhesions. Scale bars is 30 µm. **(D) Model showing ARHGAP42 activation by Src.** The BAR and GAP domains are inhibitory towards one another. Upon Src phosphorylation of Tyr-376 the inhibition is disrupted. Activation of the GAP domain leads to a decrease of RhoA-GTP levels and subsequently to lowering of acto-myosin tension, increased focal adhesion dynamics and loss of stress fibers.